Scientia Iranica B (2011) 18 (3), 383–392

Sharif University of Technology
Scientia Iranica
Transactions B: Mechanical Engineering
www.sciencedirect.com

Quantitative verification of the morphing evolutionary structural optimization method for some benchmark problems using a new performance index

H.R. Ghaffarianjam *, **M.H. Abolbashari**, **A. Farshidianfar**

Department of Mechanical Engineering, Ferdowsi University of Mashhad, Mashhad, P.O. Box 91775-1111, Iran

Received 22 November 2010; revised 22 February 2011; accepted 19 April 2011

KEYWORDS
Morphing evolutionary structural optimization;
Optimality criteria;
Stiffness;
Frequency;
Weight minimization;
Performance index.

Abstract Morphing Evolutionary Structural Optimization (MESO) is a soft-kill version of Evolutionary Structural Optimization (ESO). This paper proposes a new optimality criteria-based performance index for monitoring the optimization process of the conventional MESO method. Also, a quantitative verification of the MESO for some benchmark problems with equality constraints is presented. For some structures like Michell trusses, a qualitative verification of the ESO method has been already reflected in the literature. However, in this study, a quantitative verification of the MESO method in the shape optimization is shown by comparing the results with analytical solutions. An excellent convergence of the MESO method in stiffness, frequency and weight optimization problems with equality constraints to optimum clearly reveals that this method is a robust optimization technique, which can be easily implemented and applied to a wide range of problems.

1. Introduction

The available literature reflects that several approaches have been used for shape optimization. These approaches include microstructure-based methods, such as homogenization [1], the Solid Isotropic Microstructure with Penalty (SIMP) [2] and those based on macrostructures, such as the Soft-Kill Option (SKO) [3] and the ESO [4].

The ESO method was initially proposed by Xie and Steven [5] in 1992. This method is based on the idea of gradually removing inefficient material from an initially over-sized domain. The early version of ESO was not formulated in the conventional form of optimization problems, but a conventional form for the ESO was suggested by Querin [6]. His other great contribution was the introduction of Bidirectional Evolutionary Structural Optimization (BESO) and a new concept of soft killing or "Morphing". The ESO is classified as a hard kill method in which inefficient elements are completely removed from the structure. The MESO is a soft kill version of the ESO in which the dimensions of elements are altered in such a way that the structure converges to its optimum shape. In a typical MESO method, the initial discretized space or dimensions are first set at their reasonable maximum values. Then, based on the sensitivity number of elements, inefficient material is removed from the structure by decreasing element sizes.

The efficiency of the material layout of a structure is usually quantified and measured by a performance index. Querin [6] proposed a performance index for optimization of Michell type problems. Liang et al. [7–9] introduced a performance index for optimization problems with displacement constraints. Also, Chu et al. [10,11] suggested an optimality-based performance index for optimization problems with displacement or volume constraints.

In the past decade, particular attention has been paid to structural optimizations using the ESO approach. Although Tanskanen [12] investigated the theoretical aspects of the ESO for pin jointed structures, a precise theoretical base or detailed mathematical proof has not been established for this method yet. For some structures, like Michell trusses, a qualitative verification of the ESO has been presented in the literature by visual comparisons of the ESO results with the optimum shapes [4].

* Corresponding author.
E-mail address: Ghaffarian_jam@yahoo.com (H.R. Ghaffarianjam).

1026-3098 © 2011 Sharif University of Technology. Production and hosting by Elsevier B.V. Open access under CC BY license.
Peer review under responsibility of Sharif University of Technology.
doi:10.1016/j.scient.2011.05.028

Production and hosting by Elsevier
ELSEVIER

However, very limited quantitative verifications of the ESO are available. Since there is not much work reported for the quantitative verification of the ESO-based methods, this paper aims at investigation of the quantitative verification of the MESO method for some benchmark problems in shape optimization. In the present study, firstly, a new optimality criteria-based performance index is proposed and then a series of problems for weight, stiffness, deflection and frequency optimization of structural elements like bar, beam and plate, subject to equality constraints are studied. By quantitative, it is meant that the solutions are compared with analytical solutions. Therefore, the benchmark problems have been limited to those with their analytical solutions available. Furthermore, the convergence and monitoring of the optimization process are enhanced by introducing a proper and new performance index.

2. Performance index formulations

Generally, for an optimization problem with an equality constraint as:

$$\min: \ f(z^i), \tag{1}$$

$$\text{subject to}: \ \Psi(z^i) \equiv 0, \tag{2}$$

the Lagrange function, Φ, can be defined as:

$$\Phi(z^i, \lambda) = f(z^i) + \lambda \Psi(z^i), \tag{3}$$

where f is the objective function, Ψ is the equality constraint, z^i are the design variables, and λ is the Lagrange multiplier. Optimality conditions for this problem may be written as:

$$\frac{\partial \Phi}{\partial z^i} = 0, \quad i = 1, \ldots, n_e, \tag{4}$$

$$\frac{\partial \Phi}{\partial \lambda} = 0, \tag{5}$$

where n_e is number of design variables. Now, Eq. (4) becomes:

$$\frac{\partial f}{\partial z^i} + \lambda \frac{\partial \Psi}{\partial z^i} = 0, \quad i = 1, \ldots, n_e. \tag{6}$$

Thus the optimality conditions may be written as:

$$g_i = \frac{\frac{\partial f}{\partial z^i}}{\frac{\partial \Psi}{\partial z^i}} = -\lambda. \tag{7}$$

For small enough Δz^i, Eq. (7) may be replaced with:

$$g_i = \frac{\frac{\Delta f}{\Delta z^i}}{\frac{\Delta \Psi}{\Delta z^i}} = -\lambda, \tag{8}$$

or:

$$g_i = \frac{\Delta f}{\Delta \Psi} = -\lambda, \tag{9}$$

where Δf and $\Delta \Psi$ are the variations of f and Ψ, due to the variations of z^i. Eq. (9) states that in the optimum design, the values of g_i must be identical. Numerically, if the variance of g_i becomes small enough, the design may be regarded as an optimum.

The MESO process is based on an iterative process. In this paper, the variance of g_i is used as the optimization criterion. The variance of g_i is defined as:

$$T_j = \sqrt{\frac{\sum_{i=1}^{n_e} (g_i - \Gamma)^2}{n_e}}, \tag{10}$$

where Γ is the average of g_i in the jth iteration. A performance index for this problem can be defined as:

$$\mathrm{PI} = \frac{T_j}{T_1}, \tag{11}$$

where T_1 and T_j are the values of T for the structure in the initial state and at the jth iteration. The proposed *PI* is a dimensionless scalar number. The higher the value of T, the larger the variance of g_i. Also, a small value of T shows the uniformity of g_i. Therefore, the optimum design can be identified by minimization of *PI*.

3. Numerical examples

3.1. Fundamental frequency maximization

3.1.1. Problem definition

Shape optimization problems in which natural frequencies appear in the objective or constraint functions have received much attention in the literature. Grandhi [13] provided a good classification of the different algorithms and applications used in this field. Also, Zhao et al. [14] used the ESO method for maximizing the natural frequencies of the bending vibration of thin plates. The studied problems here are the maximization of the fundamental frequency of structures subject to constant volume. Bar and beam structures are considered in this section.

3.1.2. Sensitivity numbers

In finite element analysis terminology, the dynamic behavior of a structure is governed by [4]:

$$([K] - \omega_n^2 [M])\{u_n\} = 0, \tag{12}$$

where $[K]$ is the global stiffness matrix, $[M]$ is the global mass matrix, ω_n is the angular velocity of the nth natural frequency and $\{u_n\}$ is the eigenvector corresponding to ω_n. Two sensitivity numbers for increasing and decreasing the design variables may be defined as [4]:

$$(\alpha_n^i)^+ = \frac{1}{m_n}\{u_n^i\}^T (\omega_n^2 [\Delta M^i]^+ - [\Delta K^i]^+)\{u_n^i\}, \tag{13}$$

$$(\alpha_n^i)^- = \frac{1}{m_n}\{u_n^i\}^T (\omega_n^2 [\Delta M^i]^- - [\Delta K^i]^-)\{u_n^i\}, \tag{14}$$

in which $\{u_n^i\}$ is the eigenvector of the ith element and:

$$\begin{aligned}[\Delta K^i]^+ = {} & [K^i(z^1, z^2, \ldots, z^i + C, \ldots)] \\ & - [K^i(z^1, z^2, \ldots, z^i, \ldots)],\end{aligned} \tag{15}$$

and:

$$\begin{aligned}[\Delta K^i]^- = {} & [K^i(z^1, z^2, \ldots, z^i - C, \ldots)] \\ & - \left[K^i(z^1, z^2, \ldots, z^i, \ldots)\right],\end{aligned} \tag{16}$$

where z^i are the dimensions of the ith element, $[K^i]$ and $[M^i]$ are the stiffness and mass matrices of the ith element, respectively, C is the maximum allowable change of the design variables. Also, $[\Delta M^i]$ is calculated similar to that of $[\Delta K^i]$ in Eqs. (15) and (16), and m_n is evaluated as:

$$m_n = \{u_n\}^T [M]\{u_n\}. \tag{17}$$

These sensitivity numbers are indicators of changing ω_n as the result of altering the ith element.

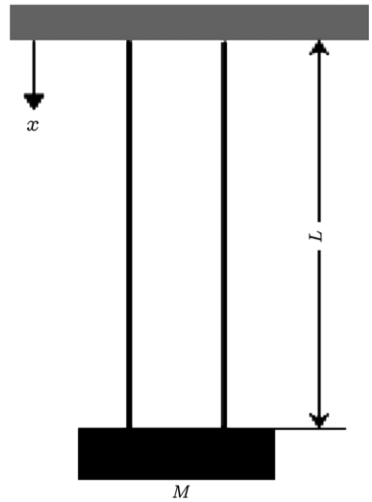

Figure 1: A vertical elastic bar with a mass.

3.1.3. Bar design for maximum fundamental frequency

A vertical elastic bar of constant volume, V_0, and variable cross sectional area, $A(x)$, is fixed at the upper end, $x = 0$, and carries a given mass, M, at $x = L$, as shown in Figure 1. The bar should be designed, such that its fundamental frequency of longitudinal vibrations becomes maximum. Thus, the problem may be formulated as:

$$\max: \ f, \tag{18}$$

$$\text{subject to}: \ \Psi \equiv V - V_0 = 0, \tag{19}$$

where f is the fundamental frequency of the bar. If the longitudinal displacement is denoted by $u(x)$, the optimality condition is [15]:

$$K_1 \equiv \left(\frac{\mathrm{d}}{\mathrm{d}x}[u(x)]\right)^2 - \frac{\omega^2}{c^2}[u(x)]^2 = \text{Constant}, \tag{20}$$

where K_1 is the numerical value of the optimality condition, ω is the angular velocity of the first natural frequency and c is the speed of the propagation of longitudinal waves in the bar, which is defined as:

$$c = \sqrt{\frac{E}{\rho}}, \tag{21}$$

where E and ρ are the elastic modulus and density of the material, respectively.

To implement the MESO, a uniform bar is considered and divided into n_e equal elements along its length, where the first element is located at the top of the bar. Design variables are the cross sectional areas of the elements of the bar. $(\alpha_n^i)^-$ and $(\alpha_n^i)^+$ are now calculated for all elements. Q elements with lowest $(\alpha_n^i)^-$ are nominated for area decrease and Q other elements with highest $(\alpha_n^i)^+$ are nominated for area increase. The value of C should be chosen, such that a small fraction of the structural volume, say 1%, is reduced in each iteration.

In this MESO procedure, the values of $\Delta\Psi$ are identical for all elements, therefore, referring to Eq. (9), the uniformity of Δf leads to the uniformity of g_i.

Since the values of m_n in Eqs. (13) and (14) are identical for all elements, these equations can be simplified by omitting m_n, as suggested in [4]. The values of the parameters are given in Table 1, where A_0 is defined as the cross sectional area of the initial uniform bar. It should be noted that the stop criterion for the optimization process is defined as:

$$\left|\frac{f(i+1) - f(i)}{f(i)}\right| < \varepsilon, \tag{22}$$

where ε is a small positive number and $f(i)$ is the value of the objective function at the ith iteration. Optimum results are displayed in Table 2. It is seen that the first natural frequency is increased by 6.23% after 52 iterations.

The analytical optimum profile of the bar has been determined in [15]. The optimum profile using the MESO and the analytical method are depicted in Figure 2, where an excellent agreement between them is observed. Also, the values of K_1 of elements of the initial and optimum bar are shown in Figure 3. It is seen that for the optimum solution obtained by the MESO, the values of K_1 in all elements are more or less identical. Figure 4 shows the evolution of PI and R. Parameter R is defined as:

$$R = \frac{f(i)}{f(1)}. \tag{23}$$

It is observed that the fundamental frequency increases with a decreases in PI. It means that as the MESO process proceeds, the criterion (9) is simultaneously satisfied, which is also a measure of the MESO performance. Figure 5 shows the values of $(\alpha_n^i)^+$ for the elements in the initial (uniform) and optimum designs. These values for the optimum design obtained by the MESO are almost identical.

Table 1: The values of parameters used in the frequency maximization of the bar.

L	1 (m)
A_0	25 (cm^2)
M	10 (kg)
n_e	100
E	210 (GPa)
ρ	7800 (kg/m^3)
C	31.25 (mm^2)
Q	20
ε	1e−4

Table 2: Numerical results for frequency optimization of the bar.

Initial bar frequency	882.99 (s^{-1})
Optimum bar frequency	938.02 (s^{-1})
Frequency increase	6.23%
No. of iterations	52

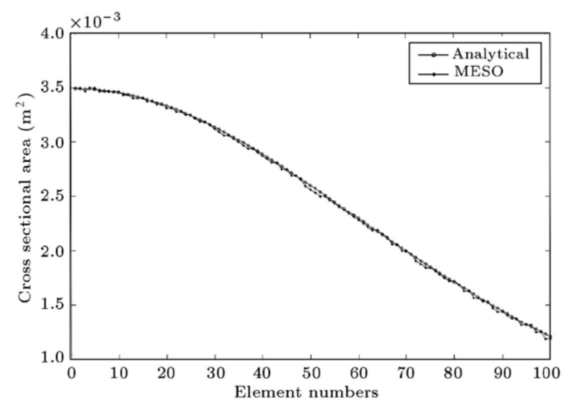

Figure 2: The analytical and numerical (MESO) cross sectional areas of elements of the optimum bar.

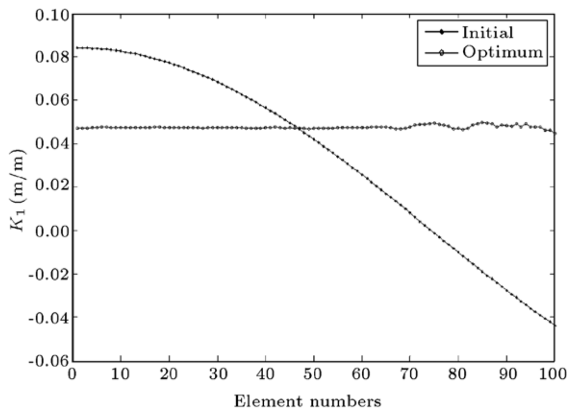

Figure 3: The values of K_1 for frequency maximization for the initial (uniform) and the optimum bar.

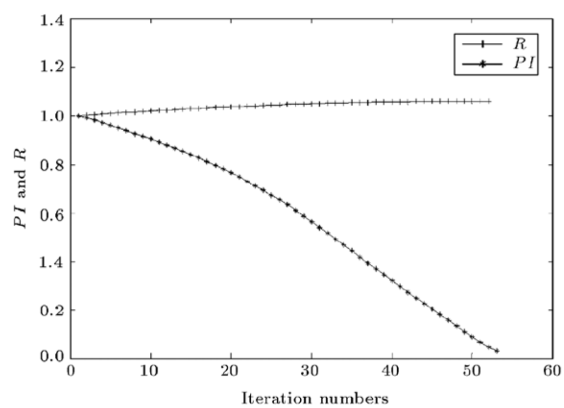

Figure 4: Evolution of *PI* and *R* for frequency maximization of the bar.

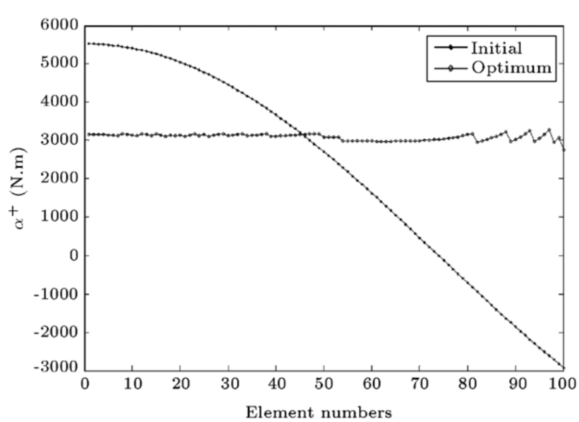

Figure 5: The values of $(\alpha_n^i)^+$ for the initial and optimum designs for frequency maximization of the bar.

3.1.4. Beam design for maximum fundamental frequency

In this section, the benchmark example is maximization of the fundamental frequency of a freely vibrating Euler–Bernoulli cantilever beam of constant volume, V_0, as shown in Figure 6. This beam has a rectangular cross section. The height of the beam (h) is held constant and its width (b) could vary. This problem may be formulated as:

$$\max: \; f, \tag{24}$$

$$\text{subject to}: \; \Psi \equiv V - V_0 = 0, \tag{25}$$

where f is the fundamental frequency of the beam.

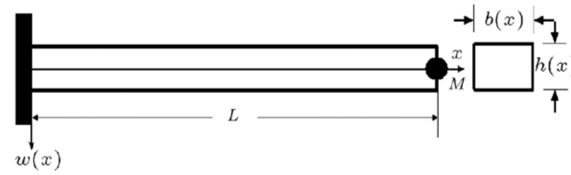

Figure 6: A cantilever beam with a concentrated mass at the tip.

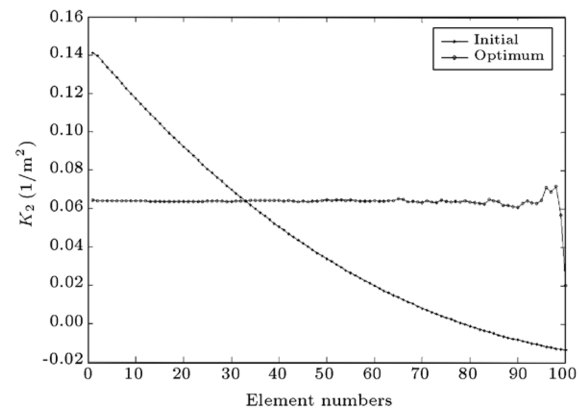

Figure 7: The values of K_2 for frequency maximization of the initial (uniform) and the optimum beams.

Table 3: The values of parameters used in the frequency optimization of the beam.

L	1 (m)
b	0.05 (m)
h	0.05 (m)
M	60 (kg)
$\boldsymbol{n_e}$	100
E	210 (GPa)
$\boldsymbol{\rho}$	7800 (kg/m^3)
C	$b/80$
Q	30
$\boldsymbol{\varepsilon}$	1e−4

Table 4: Results of frequency maximization of the beam shown in Figure 6 obtained using the MESO.

No. of iterations	Initial frequency (s^{-1})	Optimal frequency (s^{-1})	Increase (%)
78	11.34	13.45	18.61

The necessary and sufficient optimality condition may be stated as follows [15]:

$$K_2 \equiv u''^2 - \eta^2\omega^2u^2 = \text{Constant}, \tag{26}$$

where u is the transverse displacement of the beam and:

$$\eta^2 = \frac{12\rho}{Eh^2}. \tag{27}$$

In order to implement the MESO, the beam is divided into n_e equal elements along its length, where the first element is located at the clamped end. The widths of elements are taken as design variables. The values of parameters are given in Table 3 and optimization results are presented in Table 4. It is seen that the value of the fundamental frequency is increased by about 18%. Also, the values of K_2 of elements for the initial and optimum beams are shown in Figure 7. It is observed that for

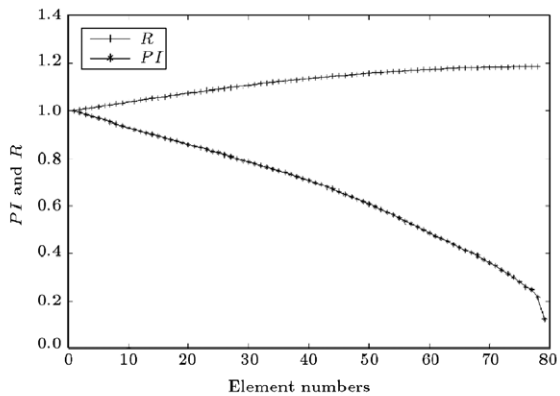

Figure 8: Evolution of *PI* and *R* for frequency maximization of the beam.

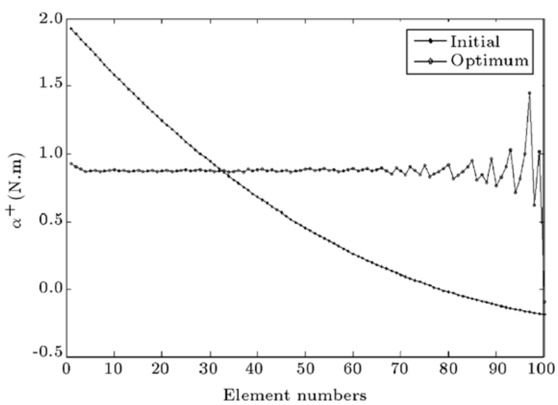

Figure 9: The values of $(\alpha_n^i)^+$ for the initial and optimum designs for frequency maximization of the beam.

the optimum solution obtained by the MESO, the values of K_2 of all elements are more or less identical. Due to introducing a lower bound on the design variables, the identity of the K_2 at the very end elements has been lost. Figure 8 displays the evolution of *PI* and *R*. Again, it is seen that the fundamental frequency increases with a decreases in *PI*, which is a measure of the MESO performance. Figure 9 shows the values of $(\alpha_n^i)^+$ for the elements in the initial and optimum designs. Once more, it is clear that these values for the optimum design obtained by the MESO are almost identical.

3.2. Design for minimum overall deflection

3.2.1. Problem definition

An elastic rectangular cantilever beam of length *L*, which is fixed at $x = 0$ and is subjected to a transverse distributed load, is considered. While the volume of the beam is held constant the objective is to minimize, f, the total transverse displacement, u, of the beam. The problem is stated as:

$$\min: \; f = \int_0^L u(x)\mathrm{d}x, \tag{28}$$

$$\text{subject to}: \; \Psi \equiv V - V_0 = 0, \tag{29}$$

where V is the volume of the beam and V_0 is a constant. Makky et al. [16] solved this problem analytically. Also, a numerical approach for this problem has been proposed in [17]. We treat the problem numerically using the MESO method and employing appropriate sensitivity numbers.

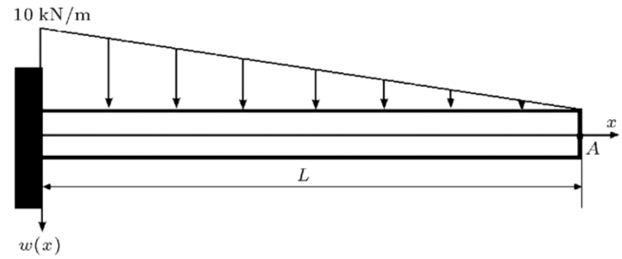

Figure 10: A rectangular cantilever beam.

For a rectangular cross sectional beam, the moment of inertia function, $I(x)$, is related to the cross sectional area function as:

$$I(x) = \gamma[A(x)]^n, \tag{30}$$

where γ is a constant related to some physical dimensions of the cross section and n is a constant that depends on the physical relation of width and height functions. If the width varies along the length but the height is constant, then $n = 1$. If the height varies along the length but the width is constant, then $n = 3$, and if the width and height both vary along the length but the width to height ratio is constant, then $n = 2$.

3.2.2. Sensitivity numbers

Using finite element analysis terminology, the static behavior of a structure is represented as:

$$[K]\{u\} = \{P\}, \tag{31}$$

where $[K]$ is the global stiffness matrix, $\{u\}$ is the nodal displacement vector and $\{P\}$ is the nodal load vector. The change of $\{u\}$ may be stated as [4]:

$$\{\Delta u\} = -[K]^{-1}[\Delta K]\{u\}. \tag{32}$$

To define the effect of changing element dimensions on the deflection integral of the beam, a load vector $\{F\}$ is introduced in which only its first and last components are equal to 0.5, while all other components are equal to unity. Multiplying Eq. (31) by $\{F\}^T$ gives:

$$\begin{aligned}\{F\}^T\{\Delta u\} &= 0.5\Delta u^1 + \Delta u^2 + \Delta u^3 + \cdots + \Delta u^{n_e-1} \\ &\quad + 0.5\Delta u^{n_e} = \Delta f \\ &= -\{F\}^T[K]^{-1}[\Delta K]\{u\} \\ &= -\{u'\}^T[\Delta K]\{u\},\end{aligned} \tag{33}$$

where $\{u'\}$ and $\{u\}$ are the solutions of Eq. (31) for the virtual load $\{F\}$ and real load $\{P\}$, respectively. Therefore, to determine the effect of the dimension change of the ith element on f, two sensitivity numbers may be defined as:

$$(\alpha^i)^+ = -\{u'\}^T[\Delta K^i]^+\{u\}, \tag{34}$$

and:

$$(\alpha^i)^- = -\{u'\}^T[\Delta K^i]^-\{u\}, \tag{35}$$

where $[\Delta K^i]^+$ and $[\Delta K^i]^-$ are defined as Eqs. (15) and (16). These sensitivity numbers can be used for evaluating the change of the deflection integral of the beam, due to the change of design variables.

Table 5: The values of parameters used in overall deflection minimization of the beam.

$\boldsymbol{L}$	1.0 (m)
$\boldsymbol{b}$	0.05 (m)
$\boldsymbol{h}$	0.05 (m)
$\boldsymbol{n_e}$	100
$\boldsymbol{C}$	$V_0/4000$ (m^3)
$\boldsymbol{Q}$	30
$\boldsymbol{E}$	210 (GPa)
$\boldsymbol{\varepsilon}$	1e−4

Table 6: The values of f_0/f^* obtained using the MESO and the analytical solutions for overall deflection minimization of the cantilever beam with the linear load for different values of n.

n	No. of Iterations	f_0/f^*		Difference (%)
		MESO	Analytical	
1	78	2.02	2.04	0.98
2	56	3.11	3.16	1.58
3	47	4.18	4.27	2.11

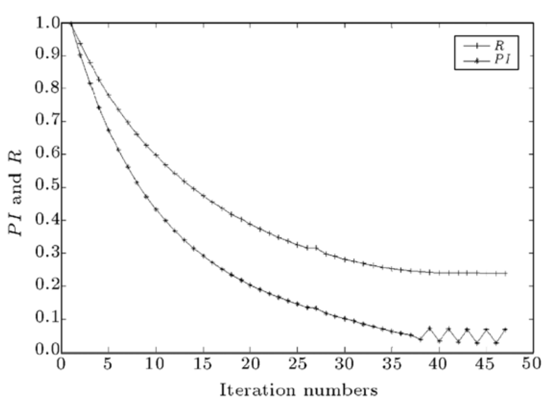

Figure 11: Evolution of *PI* and *R* for overall deflection minimization of the beam for $n = 3$.

3.2.3. Design of a cantilever beam for minimum overall deflection

A rectangular cantilever beam with a linear load is considered, as shown in Figure 10. Design variables are the cross sectional areas of the beam elements. Some problem data are given in Table 5. The ratios of deflection integral of the initial uniform shapes (f_0) to the deflection integral of the optimum shapes (f^*), using the MESO and the analytical solutions for different values of n, are displayed in Table 6. It is seen that the MESO results are very close to that of analytical solutions and the maximum difference is 2.11%, which occurs for $n = 3$. The percentage of difference is evaluated as:

$$\text{Difference} = \frac{\Omega_{\text{Analytical}} - \Omega_{\text{MESO}}}{\Omega_{\text{Analytical}}} \times 100, \tag{36}$$

where Ω is the variable that is being compared.

Figure 11 displays the evolution of *PI* and *R* for $n = 3$. It is seen that as the objective function increases, *PI* decreases. Some deviations at the last iterations are observed in the *PI* curve, which is due to imposing a lower bound on the design variables. Figure 12 depicts the values of $(\alpha^i)^+$ for the elements in the initial and optimum design for $n = 3$. It is observed that these values are almost identical in the optimum design obtained using the MESO.

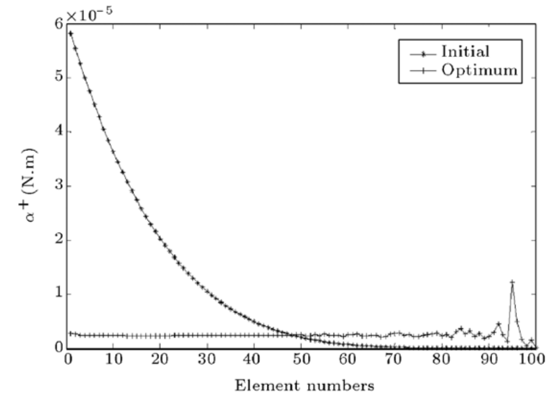

Figure 12: The values of $(\alpha^i)^+$ for the initial and optimum designs for overall deflection minimization of the beam for $n = 3$.

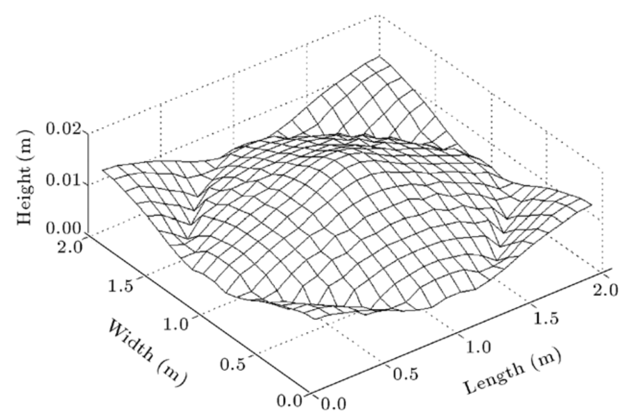

Figure 13: The height profile of the optimum plate.

3.3. Stiffness maximization

3.3.1. Problem definition

Assume a structure is being acted upon by a constant concentrated load, P, at a point, x, and the resulted displacement in the direction of the load is δ. The problem is to minimize the magnitude of δ, subject to a constraint on specific stiffness. This problem may be defined as:

$$\min:\ \delta, \tag{37}$$

$$\text{subject to}:\ \Psi \equiv \int s(x)\mathrm{d}\tau - s_0 = 0, \tag{38}$$

where $s(x)$ is the stiffness per unit length and unit area for one and two dimensional structures, respectively, τ is a nominal length or area of the structure and s_0 is a positive number. It is easy to show that a necessary and sufficient condition for optimality is [18]:

$$e(x) = \text{Constant}, \tag{39}$$

where $e(x)$ is the specific elastic strain energy or the strain energy per unit stiffness of the structure at point x.

3.3.2. Sensitivity numbers

For stiffness maximization problems, two sensitivity numbers should be defined as [4]:

$$(\alpha^i)^+ = \frac{1}{2}\{u^i\}^T[\Delta K^i]^+\{u^i\}, \tag{40}$$

$$(\alpha^i)^- = \frac{1}{2}\{u^i\}^T[\Delta K^i]^-\{u^i\}, \tag{41}$$

Table 7: The values of parameters used in the stiffness optimization of the plate.

a	2 (m)
b	2 (m)
h	1 (cm)
F	1 (kN)
ν	0.3
E	210 (GPa)
C	$D_0/20$ (N · m)
Q	64
ε	1e−4

Table 8: Results of stiffness optimization of the plate.

Central deflection of the initial plate	9.68 (mm)
Central deflection of the optimum plate	6.18 (mm)
Deflection decrease	36.16%
No. of iterations	65

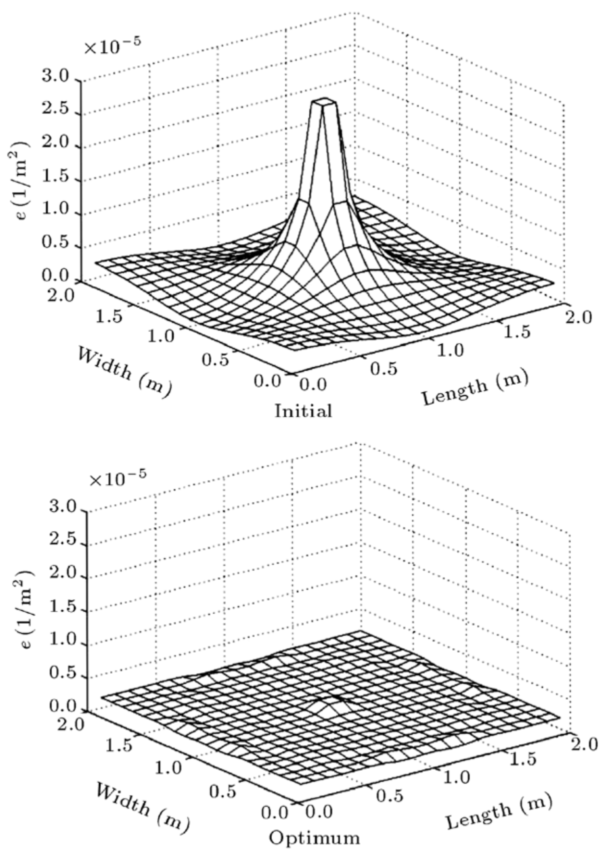

Figure 14: The specific strain energy per unit stiffness of elements for the initial (uniform) and optimum plates.

where $\{u^i\}$ is the displacement vector of the ith element. These sensitivity numbers indicate the change in the strain energy due to altering the ith element. Satisfying Eq. (38), Q elements with highest $(\alpha^i)^-$ are nominated for decreasing, and other Q elements with highest $(\alpha^i)^+$ are nominated for the increasing of their stiffness.

3.3.3. Plate design for maximum stiffness

In this case, a uniform rectangular plate with simply supported edges is examined. A concentrated force, F, is applied at the center of the plate. Suppose that a, b and h are the length, width and height of the plate, respectively. The specific stiffness

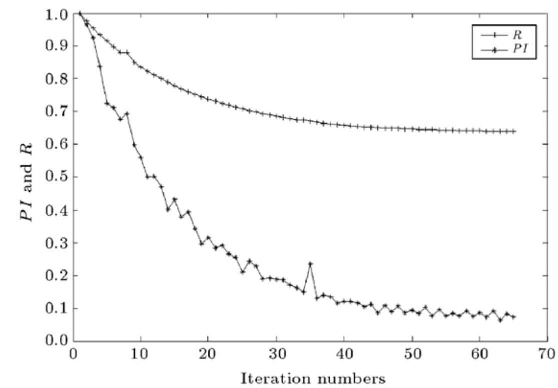

Figure 15: Evolution of PI and R for stiffness optimization of the plate.

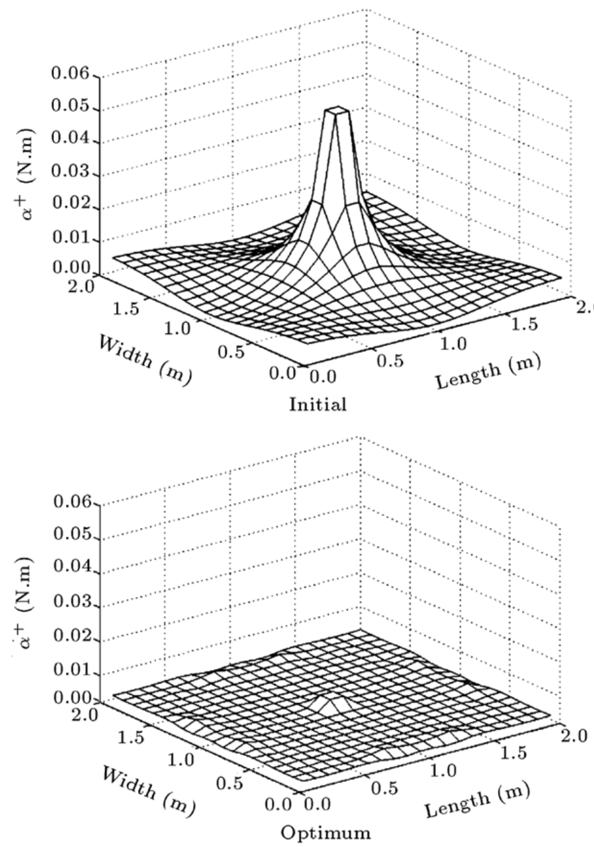

Figure 16: The values of $(\alpha^i)^+$ for the initial and optimum plates.

(or flexural rigidity) for the elastic plate is defined by D and calculated as [19]:

$$D(x, y) = \frac{Eh^3(x, y)}{12(1 - \nu^2)}, \tag{42}$$

where ν is the Poisson ratio, and $h(x, y)$ is the height profile of the plate. The flexural rigidities of elements are taken as design variables and are denoted as D. The plate geometry and other parameters are given in Table 7. The parameter D_0 in this table stands for the elemental flexural rigidity of the initial uniform plate. Due to symmetry, one quarter of the plate is analyzed and divided into 100 elements. Optimization results are presented in Table 8. It is seen that the value of the tip deflection is decreased by 36.16% after 65 iterations.

The height profile of the optimum plate using the MESO method is shown in Figure 13. The values of $e(x)$ for elements in

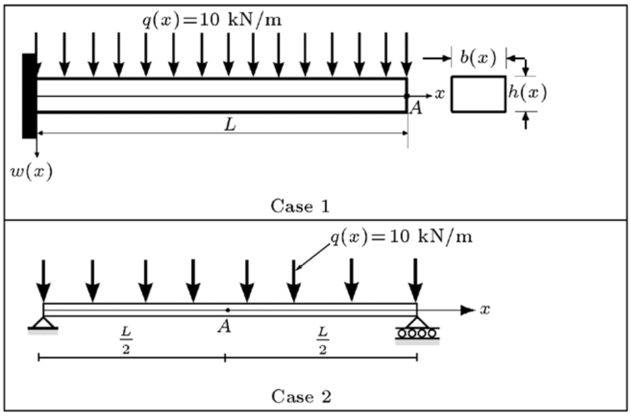

Figure 17: Geometry of rectangular beams.

the initial and optimum plates are shown in Figure 14. It is seen that for the optimum solution obtained by the MESO, the values of $e(x)$ for all elements are almost identical. The evolutions of *PI* and *R* for this problem are shown in Figure 15. It is observed that the values of *PI* decrease in a slightly coarse curve. Also, Figure 16 shows the values of $(\alpha^i)^+$ for elements in the initial and optimum design.

3.4. Minimum volume design with displacement constraint

3.4.1. Problem definition

Consider a statically determinate beam of variable cross sectional area, $A(x)$. The beam is loaded by concentrated and distributed loads and moments. The problem is defined as finding the minimum volume of the beam, such that the displacement at a specified point, $x = \xi$, be equal to a predefined value, Δ. The problem may be formulated as:

$$\min: \ V = \int_0^L A(x)\mathrm{d}x, \tag{43}$$

$$\text{subject to}: \ \Psi \equiv w(\xi) - \Delta = 0, \tag{44}$$

where V is the volume, L is the length and $w(\xi)$ is the displacement at point $x = \xi$ of the beam. This problem has been studied by several researchers [20–22].

3.4.2. Sensitivity number

Let $w(\xi)$ be the displacement of the jth element. A unit load vector, $\{F^j\}$, is introduced, in which only the jth component is non zero and equal to unity. To identify the effect of the thickness change of the ith element on $w(\xi)$, based on Eq. (31), a sensitivity number may be defined as [4]:

$$(\alpha^i)^- = |-\{u^{ij}\}^T[\Delta K^i]^-\{u^i\}|, \tag{45}$$

where $\{u^i\}$ and $\{u^{ij}\}$ are the element displacement vectors containing the entries of $\{u\}$ and $\{u^j\}$, respectively. This sensitivity number is equivalent to $\Delta\Psi$.

3.4.3. Beam design for minimum volume

To implement the MESO, a uniform rectangular beam is considered and divided into n_e equal elements along its length. The width and the height of the cross section are denoted by b and h, respectively. The volume of each element is taken as a design variable.

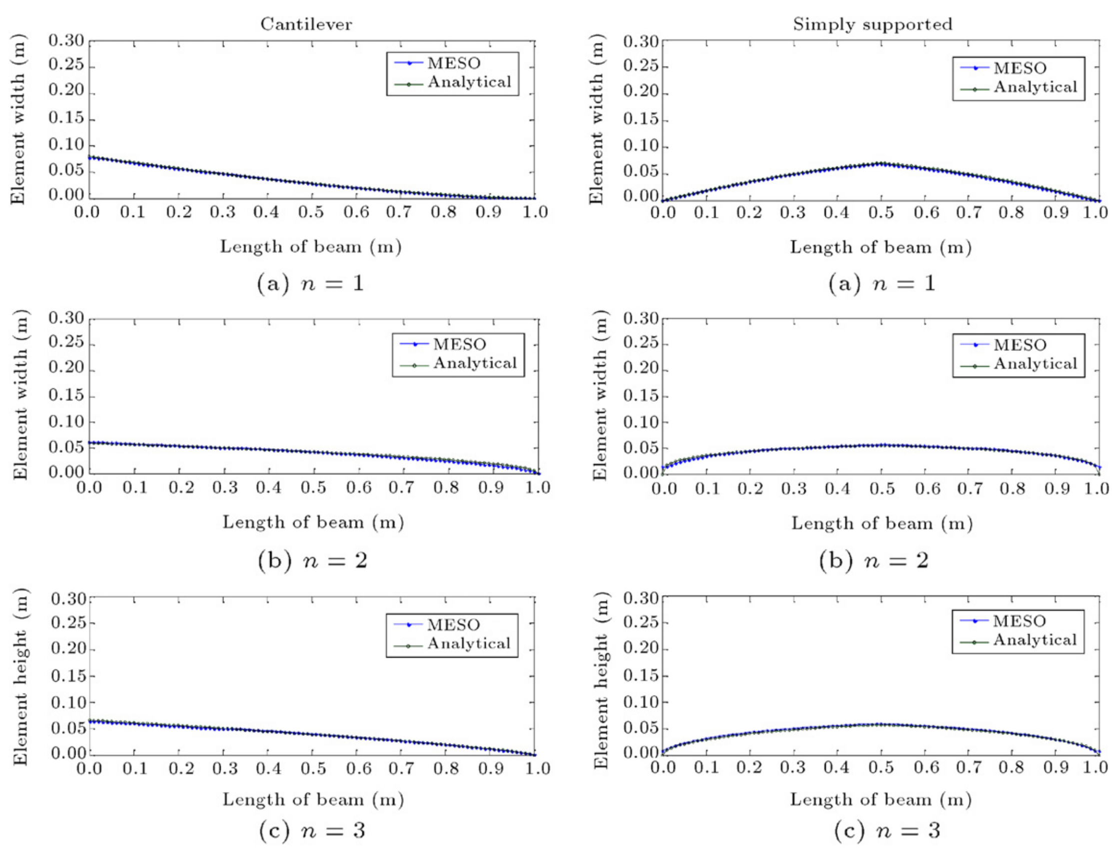

Figure 18: Optimum profiles obtained using the MESO and the analytical solution for volume minimization of beams for different values of n.

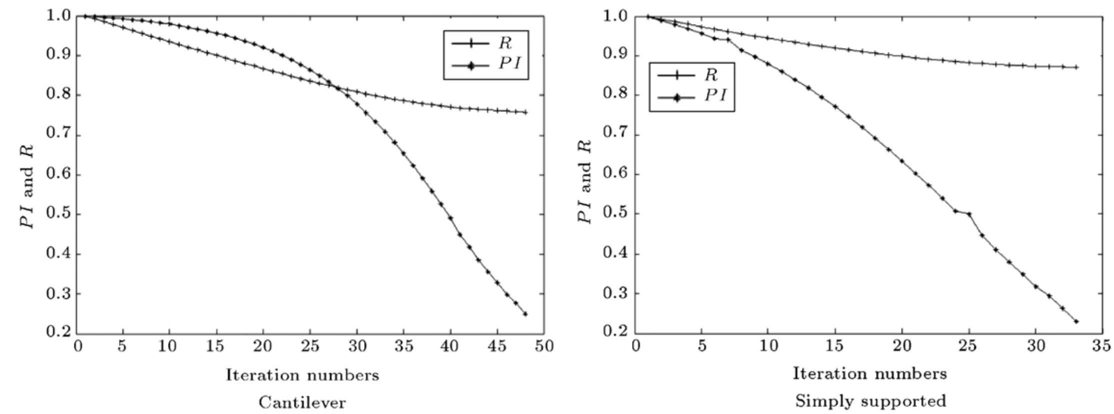

Figure 19: Evolution of *PI* and *R* for volume minimization of cantilever and simply supported beams for $n = 3$.

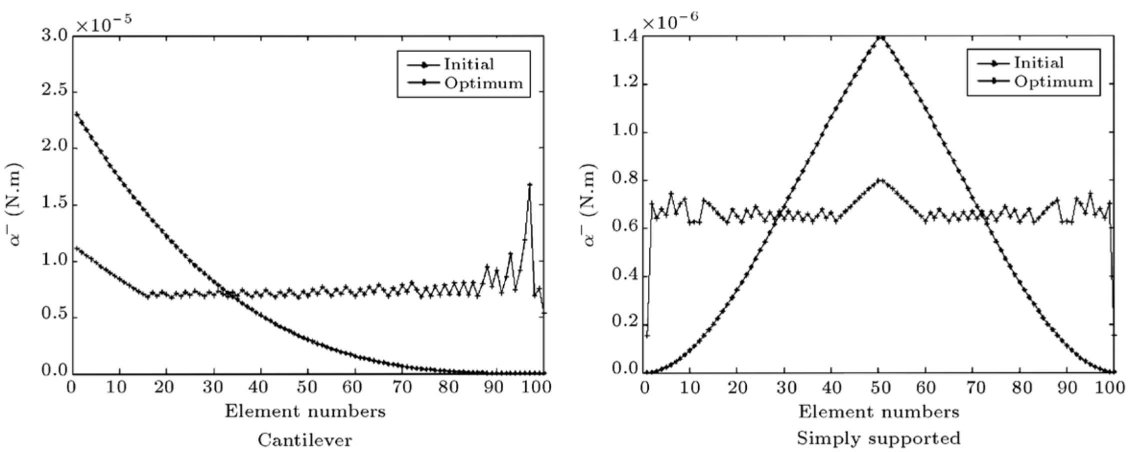

Figure 20: The values of $(\alpha^i)^-$ for the initial and optimum designs for volume minimization of cantilever and simply supported beams for $n = 3$.

In each iteration, Q elements with lowest $(\alpha^i)^-$ are selected for dimensional reduction and hence volume reduction, while an increase in $w(\xi)$ remains the least. After this, the design variables are scaled to satisfy the equality constraint [7]. The scaling procedure is accomplished by a factor of:

$$\left(\frac{\Delta}{w(\xi)_i}\right)^n, \tag{46}$$

where n is defined in Eq. (30) and $w(\xi)_i$ is the deflection of the objective point in the ith iteration. The procedure is then repeated until the stopping criterion be satisfied.

The MESO is now applied to two more cases of beams, as shown in Figure 17. In this figure, point, $x = \xi$, is denoted by A. The beam dimensions, along with n_e, Q, C and the modulus of elasticity, E, used in two cases, are given in Table 9. The volumes of optimum shapes obtained using the MESO and analytical solutions, as well as the number of iterations and the percentage of differences between volumes for different values of n, are given in Table 10.

Attention is called to the fact that in Table 10 the small values of differences (less than 1%) show the excellent convergence of the MESO method to the global optimum. Figure 18 shows the optimum beam profiles obtained using the MESO and the analytical solution. It is clear that the MESO and the analytical profiles are almost identical. The evolution of *PI* and *R* for $n = 3$ are shown in Figure 19. Also, Figure 20 shows the values of $(\alpha^i)^-$ for elements in the initial and optimum designs. It is observed that these values are different for initial beams, but eventually become more or less identical for the optimum designs.

Table 9: The values of parameters used in volume minimization of the beam.

L	1.0 (m)
b	10 (cm)
h	10 (cm)
n_e	100
C	1.25 (mm^2)
Q	30
E	300 (GPa)
ε	1e−3

Table 10: Volumes of optimum shapes obtained using the MESO and the analytical solution for different cases.

Case	Δ (mm)	n	No. of Iterations	Volume ($\times 10^{-3}$ m^3)		Difference (%)
				MESO	Analytical	
1	8.0	1	85	1.607	1.600	0.44
		2	61	1.777	1.768	0.51
		3	48	1.894	1.882	0.64
2	0.8	1	74	2.069	2.067	0.1
		2	67	2.144	2.142	0.09
		3	33	2.209	2.200	0.41

4. Conclusions

In this study, a new optimality criteria-based performance index is proposed. The method is then successfully applied to some benchmark problems. These problems are defined as finding the optimum shapes of several structural elements, while objectives are weight, stiffness, deflection and frequency. A quantitative verification of the MESO results is achieved through comparison of the results with analytical solutions. The small differences between the optimum shapes obtained analytically with those of the MESO method show an excellent convergence of the MESO algorithm to the optimum in these problems. It is observed that during the optimization process, both variance of sensitivity numbers and values of the performance index decrease. Although the present work investigates an important aspect of structural optimization, and shows the convergence of the solutions to the optimum for some structural elements, the suggested approach may be readily extended to other shape optimization problems. The presented benchmark examples only open a window to the important and interesting area of convergence of ESO-based algorithms to optimum. The subject should be explored and discussed for more complicated structures, loading and boundary conditions, as well as optimization criteria.

References

[1] Bendsøe, M.P. and Kikuchi, N. "Generating optimal topologies in structural design using a homogenisation method", *Comput. Methods Appl. Mech. Engrg.*, 71, pp. 197–224 (1988).
[2] Rozvany, G.I.N., Zhou, M. and Birker, T. "Generalized shape optimization without homogenization", *Struct. Optim.*, 4, pp. 250–252 (1992).
[3] Baumgartner, A., Harzheim, L. and Mattheck, C. "SKO (soft kill option): the biological way to find an optimum structure topology", *Int. J. Fatigue*, 14(6), pp. 387–393 (1992).
[4] Xie, Y.M. and Steven, G.P., *Evolutionary Structural Optimization*, Springer, London (1997).
[5] Xie, Y.M. and Steven, G.P. "Shape and layout optimization via an evolutionary procedure", *Proceedings of International Conference on Computational Engineering Science, Hong Kong University of Science and Technology*, Hong Kong (1992).
[6] Querin, O.M. "Evolutionary structural optimization: stress based formulation and implementation", Ph.D. Thesis, The University of Sydney, Australia (1997).
[7] Liang, Q.Q., Xie, Y.M. and Steven, G.P. "A performance index for topology and shape optimization of plate bending problems with displacement constraints", *Struct. Multidiscip. Optim.*, 21, pp. 393–399 (2001).
[8] Liang, Q.Q. and Steven, G.P. "A Performance-based optimization method for topology design of continuum structures with mean compliance constraints", *Comput. Methods Appl. Mech. Engrg.*, 191, pp. 1471–1489 (2002).
[9] Liang, Q.Q., Xie, Y.M. and Steven, G.P. "Optimal topology selection of continuum structures with displacement constraints", *Comput. Struct.*, 77, pp. 635–644 (2000).
[10] Chu, D.N., Xie, Y.M. and Steven, G.P. "An evolutionary structural optimization method for sizing problems with discrete design variables", *Comput. Struct.*, 68, pp. 419–431 (1998).
[11] Chu, D.N., Xie, Y.M. and Steven, G.P. "An evolutionary method for optimal design of plates with discrete variable thicknesses subject to constant weight", *Struct. Optim.*, 17, pp. 55–64 (1999).
[12] Tanskanen, P. "The evolutionary structural optimization method: theoretical aspects", *Comput. Methods Appl. Mech. Engrg.*, 191, pp. 5485–5498 (2002).
[13] Grandhi, R. "Structural optimization with frequency constraints—a review", *AIAA J.*, 31(187), pp. 2296–2303 (1993).
[14] Zhao, C., Steven, G.P. and Xie, Y.M. "Evolutionary natural frequency optimization of thin plate bending vibration problems", *Struct. Optim.*, 11, pp. 44–251 (1996).
[15] Prager, W. and Taylor, J.E. "Problems of optimal structural design", *J. Appl. Mech.*, 35, pp. 102–106 (1968).
[16] Makky, S.M. and Ghalib, M.A. "Design for minimum deflection", *Eng. Optim.*, 4, pp. 9–13 (1979).
[17] Ghaffarianjam, H.R. and Abolbashari, M.H. "Performance of the evolutionary structural optimization-based approaches with different criteria in the shape optimization of beams", *Finite Elem. Anal. Des.*, 46(4), pp. 348–356 (2010).
[18] Haftka, R.T. and Gürdal, Z., *Elements of Structural Optimization*, 3rd ed., Kluwer Academic Publishers, Netherlands (1992).
[19] Timoshenko, S.P. and Woinowsky-Krieger, S., *Theory of Plate and Shells*, McGraw-Hill, New York (1959).
[20] Barnett, R.L. "Minimum weight design of beams for deflection", *J. Eng. Mech. Div., ASCE*, (EM1), pp. 75–95 (1961).
[21] Shield, R.T. and Prager, W. "Optimal structural design for given deflection", *Z. Angew. Math. Phys.*, 21, pp. 513–523 (1970).
[22] Ghaffarianjam, H.R. and Abolbashari, M.H. "On the convergence of morphing evolutionary structural optimization method to the global optimum for the beam design", *Proceedings of the 8th World Congress on Structural and Multidisciplinary Optimization*, Lisbon, Portugal (June 1–5, 2009).

Hamid Reza Ghaffarianjam was born in Iran in 1974. He obtained his B.S. and M.S. degrees in Mechanical Engineering from Ferdowsi University of Mashhad, where he is currently a Ph.D. candidate in the same subject. He has co-authored more than 11 refereed journals and conference publications. His research interests include Structural Optimization Techniques.

Mohammad Hossein Abolbashari is currently Associate Professor of Mechanical Engineering at Ferdowsi University of Mashhad, Iran, where he is Director of the "Lean Production Engineering Research Center", and has recently become a faculty member of the Industrial Engineering Department. He received his Ph.D. from the University of Saskatchewan, Canada, in 1995, and has co-authored more than 50 refereed journal and conference publications. He serves on the Editorial Board of the "Journal of Applied and Computational Sciences in Mechanics" published in Farsi (Persian). He is a fellow of the Iranian Society of Mechanical Engineers (ISME) and the Iranian Organization for the Engineering Order of Buildings. His research interests include Structural Optimization, Computational Mechanics, Finite Element Methods and Time Dependent Materials.

Anooshiravan Farshidianfar is Associate Professor of Mechanical Engineering at Ferdowsi University of Mashhad, in Iran. He received his Ph.D. in Mechanical Engineering from Bradford University, UK, in 2001.

Dr. Farshidianfar has co-authored more than 114 refereed journal conference papers, besides editing, writing or contributing to 7 different books. He is a fellow of the ISME. His research interests include Vibration Analysis and Fault Diagnosis, Nonlinear Vibration and Chaos, Analysis of Chaotic Systems, Control of Vibration, Nanomechanics and Rotor Dynamics. He is currently working on Acoustics and Noise Control.